



## Modeling and Numerical Simulation of Catalytic Reforming Reactors

**REZA KHAVARI KOHNEHSHAHRI, MAHMOUD SALIMI\*,  
SEYED REZA SEIF MOHADDECY and SAEED SHIRAZIAN**

Islamic Azad University, Arak Branch, Department of Chemistry, Arak (Iran).

\*Corresponding author: E-mail: msalimi@iau-arak.ac.ir

(Received: July 20, 2011; Accepted: August 30, 2011)

### ABSTRACT

In this work, a kinetic model was developed for simulation of catalytic reforming process. The feed of catalytic reforming units is heavy naphtha including paraffin, naphthenic compounds and aromatics with 6-9 carbons. Major reactions occurred in the catalytic reactor include dehydrogenation, dehydrocyclization, isomerization, hydrocracking and ring opening. A cylindrical element of catalyst is considered to obtain conservation equations including mass and energy balances. The derived equations are solved by numerical method using MATLAB software to simulate catalytic reforming reactors. Modeling findings involving concentration, temperature and octane number variations were evaluated. Furthermore, simulation results were compared with experimental data and confirmed the accuracy of the developed model.

**Key words:** Kinetic model, Catalytic reforming process, Modeling, Numerical simulation

### INTRODUCTION

Catalytic reforming is one of the most important units of refineries. This unit is used to increase Octane number of gasoline. First catalytic reforming unit was established in the U.S. in 1939 for producing gasoline with high Octane number<sup>1</sup>. The need to upgrade naphthas was recognized early in the 20th century. Thermal processes were used first but catalytic processes introduced in the 1940s offered better yields and higher octane. The first catalysts were based on supported molybdenum oxide, but were soon replaced by platinum catalysts. The first platinum-based reforming process, UOP's Platforming™ process, came on-stream in 1949. Since the first Platforming

unit was commercialized, innovations and advances have been made continuously, including parameter optimization, catalyst formulation, equipment design, and maximization of reformate and hydrogen yields. The need to increase yields and octane led to lower pressure, higher severity operations. This also resulted in increased catalyst coking and faster deactivation rates<sup>2-5</sup>. Fig. 1 shows this unit.

Naphtha feed stocks to reformers typically contain paraffins, naphthenes, and aromatics with 6–12 carbon atoms. Most feed naphthas have to be hydrotreated to remove metals, olefins, sulfur, and nitrogen, prior to being fed to a reforming unit. A typical straight run naphtha from crude distillation

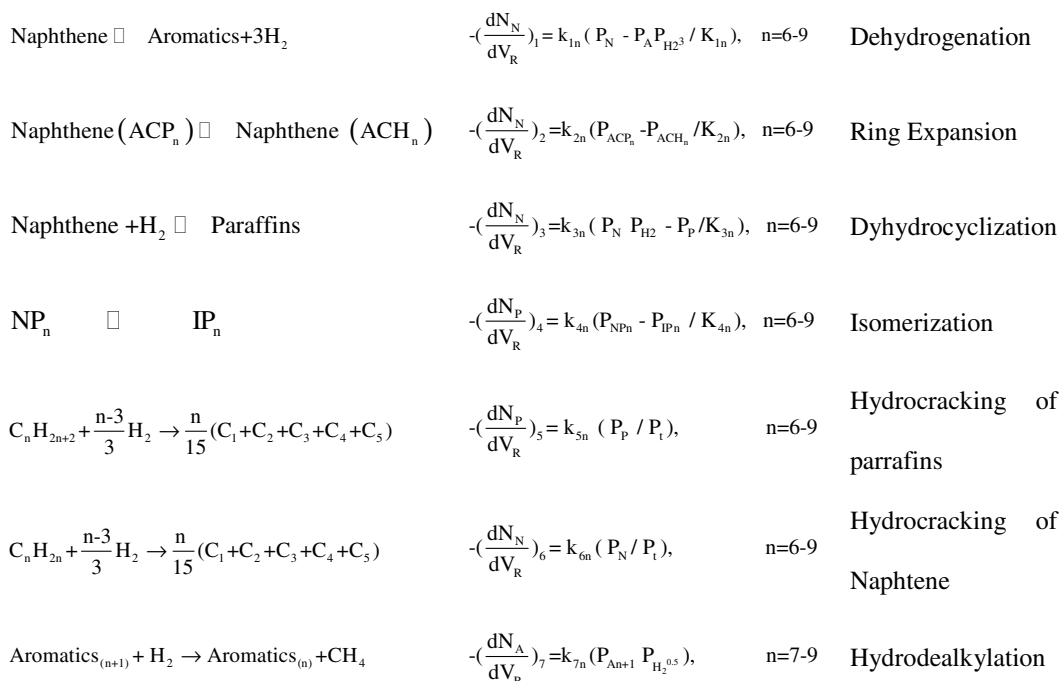
may have a boiling range of 150–400°F (65–200 °C) [6].

### Model development

The main equations that describe the

concentration distribution in the reactors are derived using mass balance around a cylindrical element in the catalyst (see figure 2). Material balances (mass balances) are based on the fundamental “law of conservation of mass”.

General chemical reactions are as below [5]



Using mass balance<sup>1</sup>

$$\frac{dN_R}{dV_R} = (r_{in} - r_{out} \pm r_{gen}) \Rightarrow \frac{dN_R}{dR} = 2\pi RL\rho_b (r_{in} - r_{out} \pm r_{gen}) \quad \dots(1)$$

$$\frac{dN_R}{dR} = 2\pi RL\rho_b \quad \dots(2)$$

$$\left(\frac{dN_A}{dV_R}\right)_t = -\left(\frac{dN_N}{dV_R}\right)_1 \pm \left(\frac{dN_A}{dV_R}\right)_7 \quad \dots(4)$$

$$\left(\frac{dN_{H_2}}{dV_R}\right)_i = -3\left(\frac{dN_N}{dV_R}\right)_1 + \left(\frac{dN_N}{dV_R}\right)_3 + \left(\frac{n-3}{3}\right)\left(\frac{dN_P}{dV_R}\right)_5 + \left(\frac{n-3}{3}\right)\left(\frac{dN_N}{dV_R}\right)_6 + \left(\frac{dN_A}{dV_R}\right)_7 \quad \dots(5)$$

Energy equation may be written as

Therefore, for all species in the reactors concentration equations are written as followings:

$$\begin{aligned} dN_{N \rightarrow An} \Delta H_{N \rightarrow An} + dN_{N(ACP_n) \rightarrow N(ACH_n)} \Delta H_{N(ACP_n) \rightarrow N(ACH_n)} + dN_{N \rightarrow P} \Delta H_{N \rightarrow P} + \\ dN_{NP_n \rightarrow IP_n} \Delta H_{NP_n \rightarrow IP_n} + dN_{PC} \Delta H_{PC} + dN_{NC} \Delta H_{NC} + dN_{A_{n+1} \rightarrow A_n} \Delta H_{A_{n+1} \rightarrow A_n} = F_t C_p dT \end{aligned} \quad \dots(6)$$

$$\left(\frac{dN_N}{dV_R}\right)_i = \left(\frac{dN_N}{dV_R}\right)_1 \pm \left(\frac{dN_N}{dV_R}\right)_2 + \left(\frac{dN_N}{dV_R}\right)_3 + \left(\frac{dN_N}{dV_R}\right)_6, \quad [+ \text{ for ACP and } - \text{ for ACH}] \quad \dots(3)$$

$$\frac{dT}{dV_R} = \sum_{n=6}^9 \sum_{i=1}^7 (-\Delta H_i) \left(\frac{dN_R}{dV_R}\right)_i \times \frac{1}{F_t C_p} \Rightarrow \frac{dT}{dR} = 2\pi RL\rho_b \left(\sum_{n=6}^9 \sum_{i=1}^7 (-\Delta H_i) \left(\frac{dN_R}{dV_R}\right)_i \times \frac{1}{F_t C_p}\right) \quad \dots(7)$$

$$C_p = a + bT + cT^2 + dT^3$$

$$\Delta H_f^\circ = a' + b'T + c'T^2 + d'T^3$$

$$\Delta G^\circ = a'' + b''T + c''T^2 + d''T^3$$

The derived equations including mass and energy equations with appropriate boundary conditions are solved numerically using codes developed in MATLAB software. The finite difference method was applied for the differential equations.

## RESULTS AND DISCUSSION

### Temperature distribution

Figure 3 illustrates temperature distribution in radial direction in three reactors of catalytic reforming process. Exothermic reactions cause temperature to increase in the reactors. The temperature increase is the highest in the first reactor. This could be related to this fact that the conversion in the first reactor is high and most reactants convert to products in the first reactor that causes the highest temperature increase in the

**Table 1: Comparison between modeling predictions and experimental data**

Parameter	Modeling	Experimental	Deviation (%)
Octane number	98.8	97.5	1.3
Efficiency	67.4	76.0	11.3

first reactor (see figure 3). The temperature increase are 50, 20 and 5 K for first, second and third reactor respectively<sup>6</sup>.

### Concentration distribution

Concentration distribution for all species is shown in figure 4. As it can be seen from the figure, hydrogen concentration decreases in the reactors. Aromatics concentration increase in the

reactors. Because of high concentration of naphthenes in the first reactor, dehydrogenation reaction is fast and the highest concentration increase is observed in this reactor. Paraffin mole fraction is almost constant in the first reactor. In the second and third reactors, paraffin mole fractions decrease because of isomerization and hydrocracking reactions.

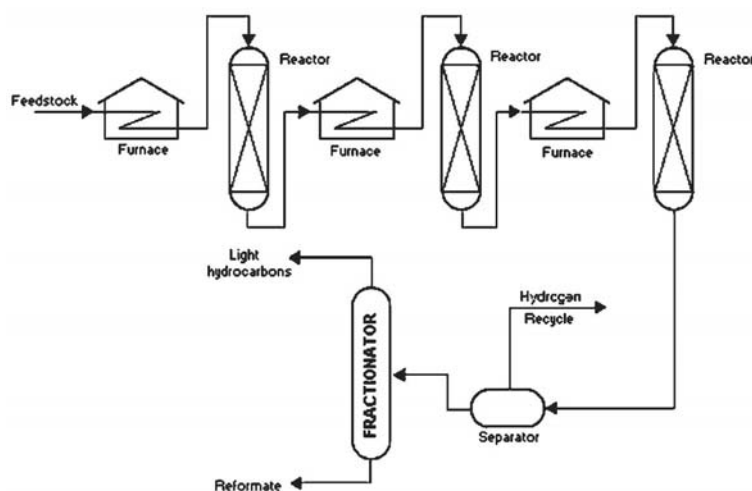


**Fig. 1: Catalytic reforming process<sup>1</sup>**

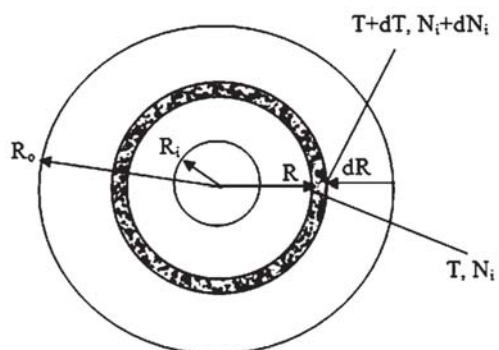


**Fig. 2:** Cylindrical element used for derivation of conservation equations

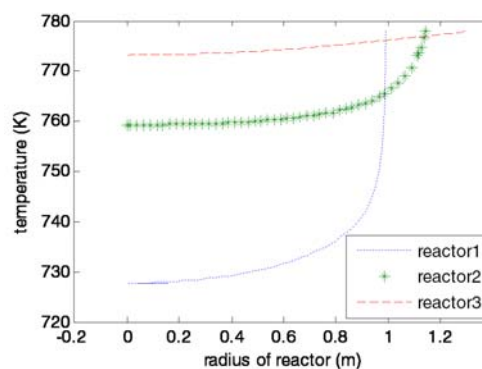


**Fig. 3:** Radial temperature distribution in the reactors

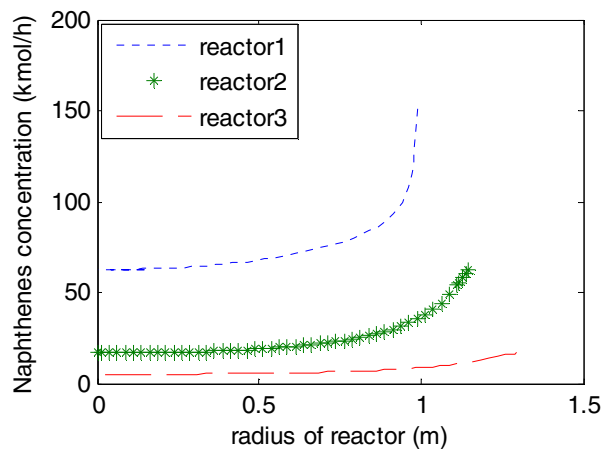
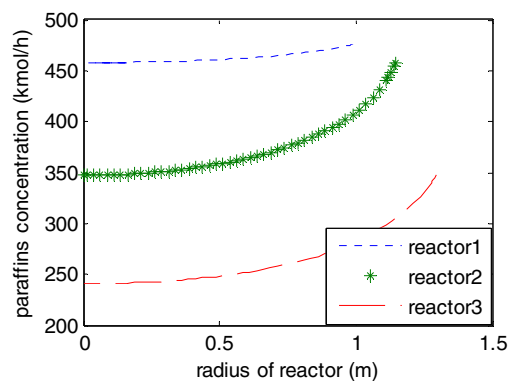
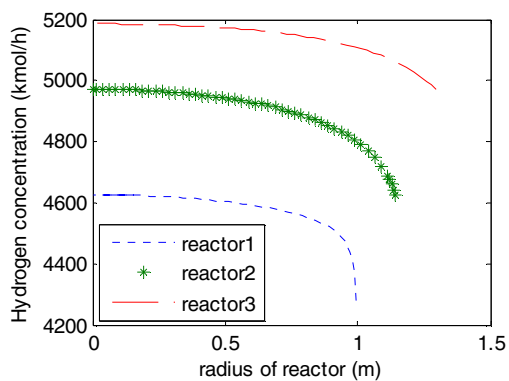


**Fig. 4:** Concentration distributions of hydrogen, aromatics and paraffin in the reactors

**Model validation**

To verify the model developed here, modeling findings were compared with the experimental data obtained from catalytic reforming unit of Tehran refinery, Iran. Table 1 shows the comparisons between experimental data and modeling findings for octane number and efficiency of catalytic reforming unit. Table 1 reveals that the model matches the experimental data well and can predict the performance of catalytic reforming process.

**CONCLUSIONS**

In this study a mathematical model was developed for simulation of catalytic reforming unit. The model was based on solving the conservation equations including mass and energy for all species in the reactors. Three reactors were considered in

series for simulation. Simulation results indicated that the highest conversion occurs in the first reactor and most species react in this reactor. Most reactions were exothermic and caused an increase in temperature. Furthermore, the modeling predictions were compared with the experimental data and were in good agreement with them.

**Nomenclature**

N	mole (mol)
R	reactor radius (m)
L	reactor length (m)
V	volume (m <sup>3</sup> )
r	radial coordinate (m)
F	molar flow rate (mol/s)
C <sub>p</sub>	heat capacity (j/mol.K)
T	temperature (K)
ρ	density (kg/m <sup>3</sup> )

**REFERENCES**

1. W. Hou, H. Su, Y. Hu, J. Chu, Modeling, Simulation and Optimization of a Whole Industrial Catalytic Naphtha Reforming Process on Aspen Plus Platform, *Chinese Journal of Chemical Engineering*, **14**: 584-591 (2006).
2. L.M. Rodríguez Otal, T. Viveros García, M. Sánchez Rubio, A model for catalyst deactivation in industrial catalytic reforming, in: C.H. Bartholomew, G.A. Fuentes (Eds.) *Studies in Surface Science and Catalysis*, Elsevier, 319-325 (1997).
3. H.O.U. Weifeng, S.U. Hongye, M.U. Shengjing, C.H.U. Jian, Multiobjective Optimization of the Industrial Naphtha Catalytic Reforming Process, *Chinese Journal of Chemical Engineering*, **15**: 75-80 (2007).
4. Enefiok Akpan, Abayomi Akande, Ahmed Aboudheir, Hussam Ibrahim and Raphael Idem, Experimental, kinetic and 2-D reactor modeling for simulation of the production of hydrogen by the catalytic reforming of concentrated crude ethanol (CRCCE) over a Ni-based commercial catalyst in a packed-bed tubular reactor, *Chemical Engineering Science* **62**(12): 3112-3126 (2007).
5. M.R. Rahimpour, D. Iranshahi, E. Pourazadi and A.M. Bahmanpour, A comparative study on a novel combination of spherical and membrane tubular reactors of the catalytic naphtha reforming process, *International Journal of Hydrogen Energy* **36**(1): 505-517 (2011).
6. A. L. Huebner, "Tutorial: Fundamentals of Naphtha Reforming," AIChE Spring Meeting Houston, TX, 14-18 (1999).